ORIGINAL PAPER

Analysis of flux footprints in fragmented, heterogeneous croplands

Shweta Kumari[1,2] · B. V. N. P. Kambhammettu[1] · Mark. A. Adams[2] · Dev Niyogi[3,4]

Abstract

An accurate quantification of fluxes from heterogeneous sites and further bifurcation into contributing homogeneous fluxes is an active field of research. Among such sites, fragmented croplands with varying surface roughness characteristics pose formidable challenges for footprint analysis. We conducted two flux monitoring experiments in fragmented croplands characterized by two dissimilar surfaces with objectives to: (i) evaluate the performance of two analytical footprint models in heterogeneous canopy considering aggregated roughness parameters and (ii) analyze the contribution of fluxes from individual surfaces under changing wind speed. A set of three eddy covariance (EC) towers (one each capturing the homogenous fluxes from individual surfaces and a third, high tower capturing the heterogeneous mixed fluxes) was used for method validation. High-quality EC fluxes that fulfill stationarity and internal turbulence tests were analyzed considering daytime, unstable conditions. In the first experiment, source area contribution from a surface is gradually reduced by progressive cut, and its effect on high-tower flux measurements is analyzed. Two footprint models (Kormann and Meixner 'KM'; analytical solution to Lagrangian model 'FFP') with modified surface roughness parameters were applied under changing source area contributions. FFP model has consistently over predicted the footprints ($\text{RMSE}_{\text{FFP}} = 0.31$ m^{-1}, $\text{PBIAS}_{\text{FFP}} = 19.00$), whereas KM model prediction was gradually changed from over prediction to under prediction towards higher upwind distances ($\text{RMSE}_{\text{KM}} = 0.02$ m^{-1}, $\text{PBIAS}_{\text{KM}} = 8.50$). Sensitivity analysis revealed that the models are more sensitive to turbulent conditions than surface characteristics. This motivated to conduct the second experiment, where the fractional contribution of individual surfaces (α and β) to the heterogeneous fluxes measured by the high tower (T3) was estimated using the principle of superposition ($\text{FT3} = \alpha\,\text{FT1} + \beta\,\text{FT2}$). Results showed that α and β are dynamic during daylight hours and strongly depend on mean wind speed (U) and friction velocity ($u*$). The contribution of fluxes from adjoining fields $[1 - (\alpha + \beta)]$ is significant beyond 80% isopleth. Our findings provide guidelines for future analysis of fluxes in heterogeneous, fragmented croplands.

✉ Shweta Kumari
  shwetasingh7892@gmail.com

1   Department of Civil Engineering, Indian Institute of Technology Hyderabad, Kandi, India

2   School of Science, Swinburne University of Technology, Melbourne, Australia

3   Department of Earth and Planetary Sciences, Jackson School of Geosciences, The University of Texas, Austin, TX 78712, USA

4   Department of Civil, Architectural, and Environmental Engineering, Cockrell School of Engineering, The University of Texas at Austin, Austin, USA

1 Introduction

Eddy covariance (EC) technique provides a direct measurement of fluxes of trace gasses (such as CO_2 and CH_4) within the atmospheric boundary layer at high temporal frequencies (Aubinet et al. 1999; Leclerc and Foken 2014b). EC techniques rely on the covariance of turbulent fluctuations between vertical wind speed and the scalar component of interest. EC methods are now a mainstay of continental and global assessments of carbon and water exchanges (Chu et al. 2021). Applications of EC have spread into many domains including dense vegetative forests (Longdoz and Granier 2012), managed agricultural croplands (Moureaux et al. 2012), grasslands (Wohlfahrt et al. 2012), wetlands (Laurila et al. 2012), inland water bodies such as lakes (Timo Vesala et al. 2012), and densely populated urban areas (Feigenwinter et al. 2012). Measured fluxes are primarily originated from an upwind

region, known as the footprint. Mathematically, flux footprints are described using functions that relate spatial distribution of surface sources/sinks to the measured signal (Horst and Weil 1992; Leclerc and Thurtell 1990). Conceptually, footprint represents the sensor's 'field of view' with size and shape depending on meteorological, and surface parameters such as measurement height, wind direction, atmospheric stability, and surface roughness (Rannik et al. 2012). An accurate representation of footprint is indispensable for many applications including data interpretation, quality assessment, and upscaling (Arriga et al. 2017; Chu et al. 2021; Göckede et al. 2004). Footprint models serve as an important first step in evaluating the contribution of different sources/sinks to the fluxes measured by EC towers.

Methods for characterizing footprint fall into four categories: (i) analytical models that are based on the solution of an advection–diffusion equation (Horst 1999; Horst and Weil 1992, 1994; Hsieh et al. 2000; Kaharabata et al. 1997; Kljun et al. 2002, 2004; Kormann and Meixner 2001; Schmid 1994; Schmid and Oke 1990; Schuepp et al. 1990), (ii) stochastic Lagrangian particle dispersion models (LS) that simulate trajectories of a large number of particles between their source and the point of measurement (Kljun et al. 2015; Markkanen et al. 2009), (iii) large-eddy simulation models that solve for flow field characteristics by neglecting small-scale information via numerical solution of Navier–Stokes equations (Markkanen et al. 2009), and (iv) ensemble average closure models that use empirical information to close sets of ensemble-averaged Navier–Stokes equations (T. Vesala et al. 2008). A comprehensive overview of footprint approaches, their applications and limitations can be derived from numerous publications (Foken and Leclerc 2004; Leclerc and Foken 2014a; Rannik et al. 2012; Schmid 2002; Vesala et al. 2008). Analytical models have relatively few parameters, computationally inexpensive, and are straightforward to use, hence widely used for footprint characterization (Leclerc and Foken 2014a). Footprints from analytical models can be estimated exclusively from the atmospheric variables (Leclerc and Foken 2014b) via model parameterization (Leclerc and Foken 2014a). However, these models consider a horizontal homogeneous field for footprint characterization (Rannik et al. 2012). To date, Korman and Meixner (KM) model is arguably the most preferred analytical solution due to its: (i) ease of use, (ii) consideration of realistic power-law profiles of eddy diffusivity and wind velocity, (iii) applicability over a wide range of stability conditions, and (iv) numerical stability (Leclerc and Foken 2014b). Reliable application of the KM model is however restricted to near-surface measurements and homogeneous surfaces. Alternatively, the flux footprint parameterization approach (FFP model) considers changes in surface roughness through a scaling approach, hence

widely used for a broad range of boundary layer conditions and measurement heights (Kljun et al. 2002, 2004, 2015).

Real-world sites are often complex and spatially heterogeneous with respect to surface characteristics such as topography, roughness length, and leaf area index. This is particularly true to Indian agro-economic settings dominated by fragmented, heterogeneous croplands. A high diversity among the agricultural fields in terms of shape, size, crops sown, management practices, etc. makes the fluxes to be highly heterogeneous. Interpretation and bifurcation of fluxes from such complex sites is highly challenging as the outreach of homogeneous surface is usually shorter than the footprint (Rannik et al. 2012). Fractional contribution of individual fields to the fluxes observed in such mixed fetch environment depends on many factors including measurement height, aerodynamic roughness, boundary layer characteristics, and atmospheric stability (Foken and Leclerc 2004; Göckede et al. 2004; Rebmann et al. 2005). While analytical models successfully represent the source area of fluxes from homogenous fields, the effect of surface heterogeneity remains mostly unexplored (Göckede et al. 2005). The ability of analytical models to simulate fluxes generated from such heterogeneous surfaces can be improved with: (i) parameter aggregation that considers arithmetic and area-weighted averages of input parameters (e.g., roughness length) from contributing homogeneous surfaces (Stull and Santoso 2000), (ii) inclusion of an effective roughness length parameter normalized with friction velocity (Göckede et al. 2004; Hasager and Jensen 1999; Taylor 1987), and (iii) flux averaging technique, that superimposes fluxes estimated from individual land-uses using tile or sub-grid scale approach (Beyrich et al. 2006; Leclerc and Foken 2014a; Wang et al. 2006).

Field validation of flux footprints over heterogeneous sites characterized by two dissimilar surfaces can be done using a set of three EC towers: two low towers capturing homogeneous fluxes from individual landscapes (as reference), and a third high tower capturing heterogeneous, mixed fluxes (Foken and Leclerc 2004). Several studies have compared the fluxes measured on a high tower with the area-averaged footprint from individual fields (Avissar and Pielke 1989). For example, Beyrich et al. (2006) developed a strategy to estimate area-averaged turbulent fluxes over a heterogeneous landscape. Sensitivity of source area to surface characteristics and atmospheric stability was analyzed using a two-dimensional footprint model (Schmid 1997) combined with EC tower data. Göckede et al. (2005) analyzed correlations between measured and model-simulated fluxes in a mixed fetch using flux source area method (FSAM) (Schmid 1994, 1997) and LS models. They concluded that a three-tower configuration (with two reference systems and one with mixed fetch) outperformed two-tower configurations (both capturing heterogeneous fluxes with varying source

strengths) for validating the footprint models in heterogeneous conditions. Arriga et al. (2017) used three EC systems to partition carbon fluxes in managed, progressively cut grasslands based on two analytical models (Schuepp and KM) and numerical LS models. They concluded that a detailed description of roughness and vertical turbulent structure would improve footprint prediction in complex topography.

An extensive literature survey using Scopus (Elsevier) database for the period 2007–2023 has resulted in 107 published articles on the application of footprints for heterogeneous landscapes. Of these, only 8 (<0.1%) articles have used analytical models to heterogeneous vegetative surfaces. Interestingly, none of these studies have considered realistic, fragmented croplands characterized by dissimilar surfaces that typify Indian agro-economic settings such as: (i) dissimilar surfaces resulting from progressive harvesting of a crop and (ii) dissimilar surfaces resulting from growing multiple crops. This study is aimed at extending the application of analytical footprint models to Indian fragmented landscapes using EC flux observation datasets. Hence, the objectives of this study are to: (i) evaluate the performance of two footprint models (KM and FFP) with modified roughness parameters to represent fluxes under changing source area and (ii) analyze the contribution of individual surfaces to the heterogeneous fluxes measured in a mixed fetch environment under changing turbulence. To achieve these objectives, two flux monitoring experiments were performed. These two experiments are akin to the commonly found mixed flux scenarios in Indian agro-economic settings. In the first experiment (successive cut experiment), vegetation cover (of sugarcane) within the source area is gradually reduced to modify surface roughness. Performance of two footprint models with modified roughness parameters was evaluated under changing source area. In the second experiment (two crop surface experiment), the fractional contribution of individual surfaces (sugarcane and cotton) to the fluxes measured in mixed fetch conditions was analyzed under changing turbulent conditions, in particular wind speed. In both experiments, carbon fluxes were monitored during daytime unstable atmospheric conditions (10:00 to 18:00 Hrs of the day). The towers were configured in such a way that one tower (T3) monitors combined fluxes from the two surfaces, while other two reference towers (T1 and T2) monitor fluxes generated from individual fields. We hypothesized that differences in measured fluxes among the towers were largely attributable to underlying surface characteristics and less attributable to errors in measurement. Flowchart illustrating the proposed methodology is presented in Fig. 1.
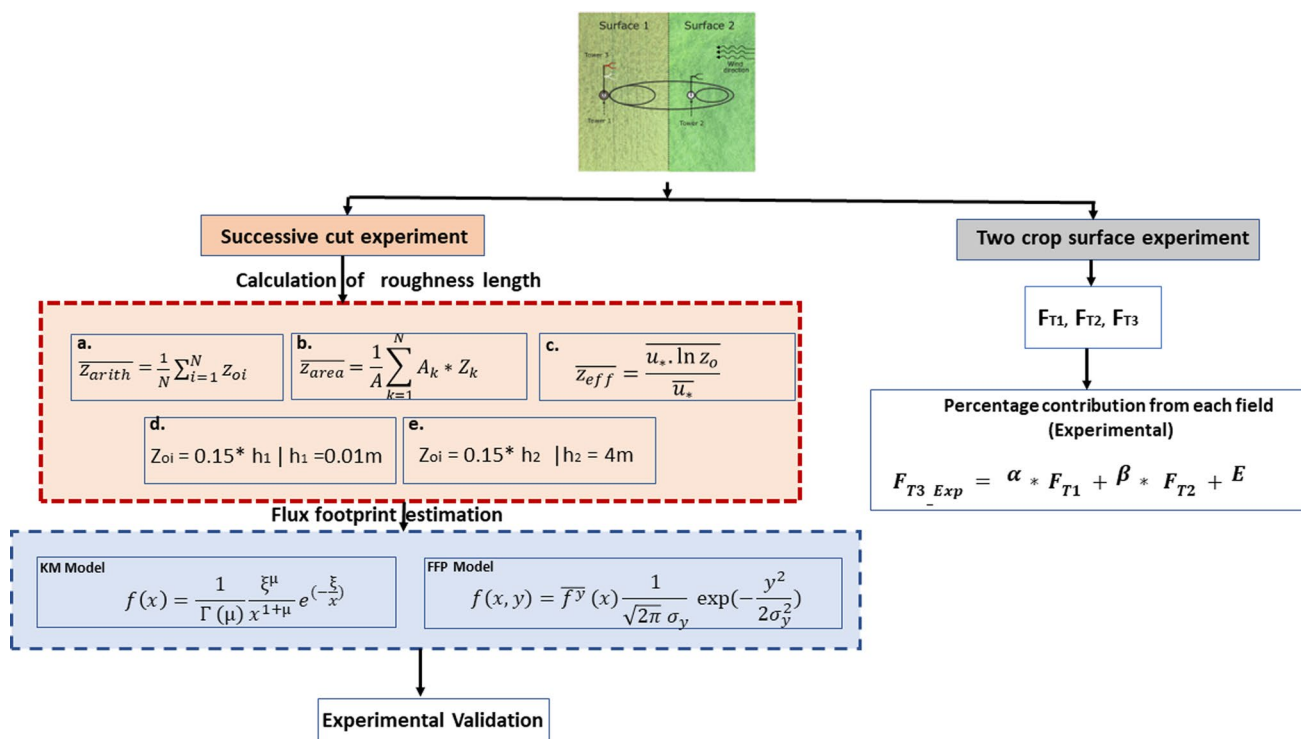

Fig. 1 Flowchart illustrating the methodology to quantify (successive cut experiment) and partition (two crop surface experiment) fluxes from fragmented, heterogeneous croplands. For a detailed explanation of the variables, the reader is advised to refer Eqs. (2)–(7)

2 Materials and methodology

2.1 Site characterization and instrumentation

Flux monitoring experiments were conducted in privately owned agricultural fields located in Nandi Kandi Village, Telangana, India (latitude: 21° 25′ 30.7″ E, longitude: 78° 9′ 30.2″ N, elevation: 534 m asl). Agricultural parcels of the region are highly fragmented with areas ranging from 0.014 to 1.3 ha. The shape, size, and orientation of the land parcels are highly non-uniform, posing challenges for data analysis and interpretation. The region has a semi-arid climate (BSh, Köppen and Geiger climate classification) characterized by hot summers and warm to cool winters with low precipitation (Köppen 1884). Average annual precipitation for the study area is 795 mm, with more than 80% received during monsoon months (Jun–Oct). Annual potential evapotranspiration (PET) for the region is 1790 mm (IMD report 1901–2017). Three EC towers, with two low height towers (T1 and T2) capturing the homogeneous fluxes from individual surfaces, and the third higher tower (T3) capturing the heterogeneously mixed fluxes forms the basis for flux monitoring. Each tower is equipped with a 3D sonic anemometer (to measure three-dimensional wind velocity) and an open-path fast response infrared gas analyzer (IRGASON-EB-IC, Campbell Sci. Inc., USA) to measure CO_2 and H_2O fluxes.

Raw data were collected with a logger (CR3000, Campbell Sci. Inc., USA) at 10 Hz frequency and averaged at half-hour intervals for computations. Wind rose diagrams for the study region reveal a prevailing South to North wind during experiment 1, and East to West flowing wind during experiment 2. All sensors were thus oriented in the predominant wind direction to minimize errors associated with flux loss (Kumari et al. 2020).

2.1.1 Successive cut experiment

The first experiment was conducted in a sugarcane field of 1.24 ha, having a long side (135 m) in the North–South direction (Fig. 2a). During the monitoring period (6–13 Jan 2018, i.e. DOY 6–13, 2018), the field was progressively cut (at 20 m per day) from South to North using a mechanical harvester to remove leafy tops and stalk, resulting in steep roughness change across the interface. Mean canopy height (hc) and roughness length (z_0) of sugarcane and cut surfaces during the monitoring period are 4.0 m, 0.6 m; and 0.01 m, 0.0015 m respectively. This will ensure a maximum possible roughness length change in managed croplands. The first ($Z_m = 6$ m) and second ($Z_m = 1.5$ m) towers were aimed to monitor homogenous fluxes from the two reference (sugarcane and mowed) surfaces. In contrast, the third tower ($Z_m = 8$ m) is aimed to monitor fluxes from the sugarcane field with a reduced source area. All fields outside the experimental setup were harvested, hence the
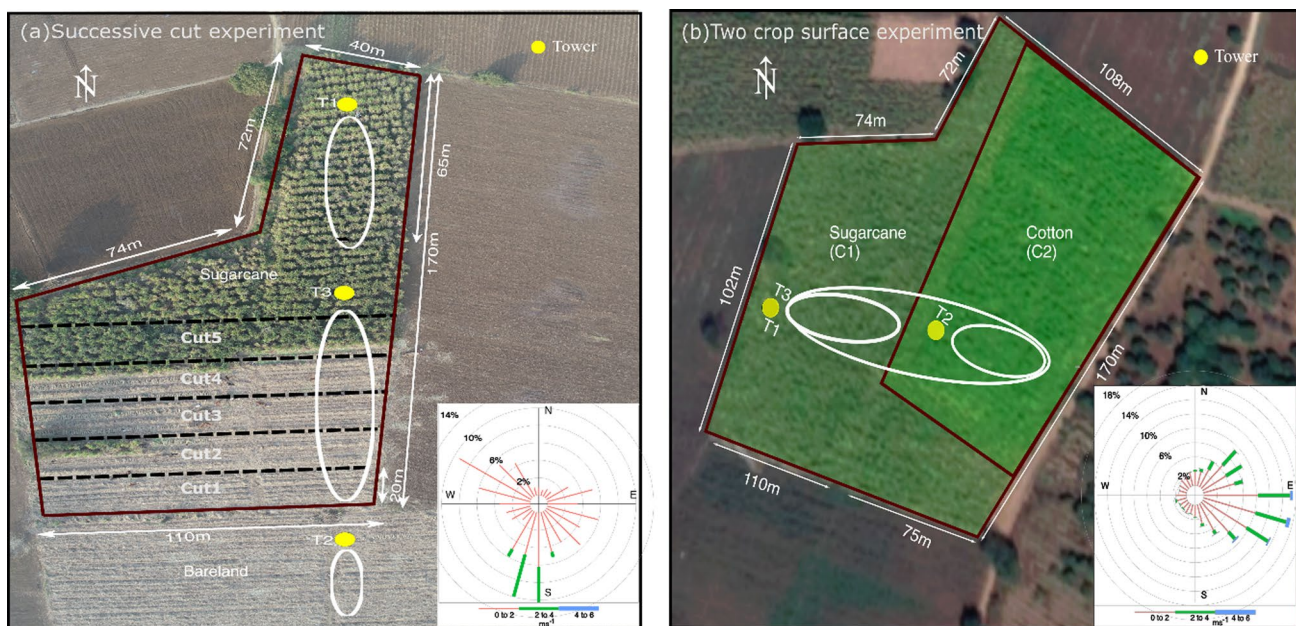

Fig. 2 Distribution of agricultural fields within the study area specific to successive cut experiment (left) and two crop surface experiment (right). Yellow dots and ovals correspond to eddy covariance (EC) flux towers and corresponding two-dimensional flux footprints under unstable atmospheric conditions. A wind rose diagram showing the predominant wind directions during the monitoring period is shown in the inset

contribution of fluxes from the nearby fields is neglected. All fluxes were observed during daytime, unstable atmospheric conditions ($u* = 0.16 \pm 0.5$ ms^{-1}, $L = -11.35 \pm 38.76$ m, $U = 0.81 \pm 0.46$ ms^{-1}).

2.1.2 Two crop surface experiment

The second experiment was conducted in a fragmented cropland characterized by two dissimilar surfaces, i.e., sugarcane–cotton (Fig. 2b). The sugarcane field (C1) has an area of 1.24 ha, mean canopy height (hc) of 4.0 m, roughness length ($z0$) of 0.6 m, and a mean leaf area index (LAI) of 3.0 m^{2}m^{-2}. Corresponding values for the cotton field (C2) are 1.21 ha, 1.5 m, 0.225 m, and 4.3 m^{2}m^{-2}. Sugarcane was planted in December 2017, whereas cotton was planted in June 2018. The monitoring period of the two crop surface experiment was (01 Apr–19 Dec, 2018 i.e. DOY: 91–353, 2018). Both fields are drip-irrigated with an average frequency of 6–8 days. Two low-height towers (T1 and T2) mounted in sugarcane ($Z_m = 6$ m) and cotton ($Z_m = 3$ m) fields were intended to capture the fluxes originating from respective fields. The third (high) tower (T3) was located in the sugarcane field ($Z_m = 8$ m) and is designed to capture the combined fluxes originating from the two fields. All sensors were aligned in East direction with fluxes observed during daytime, unstable atmospheric conditions ($u* = 0.32 \pm 0.07$ ms^{-1}, $L = -28.62 \pm -31.44$ m, $U = 0.96 \pm 0.50$ ms^{-1}).

2.2 Flux data processing and quality assessment

Eddypro post-processing software was used for primary data processing on half-hour mean fluxes (Version 6.2.0, LI-COR, USA). First, several standard corrections were applied on the fast response measurements, including: (a) removal of bad quality (quality tag > 1) data, (b) tilt corrections on sonic measurements (Wilczak et al. 2001), (c) frequency response corrections and (d) Webb–Pearman–Leuning (WPL) corrections (Ray Leuning 2007). We then applied secondary corrections to remove spurious data and fill the data gaps with reasonable estimates. The REddyproc package (Wutzler et al. 2018) developed in an open-source 'R' environment and MATLAB script were used for secondary data processing that includes: (a) flux spike removal and (b) removal of negative night time CO_2 fluxes.

To ensure the reliability of EC measurements made in a heterogeneous mixed fetch environment, we assigned quality flags to the observed CO_2 fluxes based on the deviation from ideal conditions (Foken and Wichura 1996; Göckede et al. 2004). Quality metrics considered include: (i) stationarity of measurements, and (ii) development of full-scale turbulent conditions (Göckede et al. 2004). The stationarity of flow was tested by comparing 30-min covariance with a mean of six successive sets of 5-min covariances obtained for the same period (Foken and Wichura 1996). The development of full-scale turbulent conditions was tested using flux-variance similarity theory (R. Leuning et al. 1982; Optis et al. 2014; Wyngaard et al. 1971). Turbulent characteristics of wind velocity components (u and w) were compared with values parameterized with standard functions developed for flat terrains with low vegetation (Thomas and Foken 2002). Deviations between measured and parameterized values were then used to derive an integrated quality tag for each measurement that ranged from 0 (best) to 2 (worst) (Foken and Wichura 1996; Foken et al. 2005; Göckede et al. 2008). EC fluxes with a quality tag of ≤ 1 were considered further for footprint analysis and hypothesis testing.

2.3 Footprint modeling

2.3.1 Flux footprint functions

Mathematically, flux footprint (*f*) is a transfer function between sources or sinks of passive scalars at the surface (Qc), and turbulent flux (Fc) measured at a receptor height of Z_m (Pasquill and Smith 1983; Schmid 2002). Footprint function (*f*) estimates the location and relative importance of passive scalar sources/sinks that are influencing the flux measurements (Fc) at a given receptor height (Z_m). For a receptor mounted above the origin (0, 0) with positive '*x*' indicating upwind distance, relation between fluxes measured by an EC tower (Fc) and a footprint function from analytical models (*f*) is given by:

$$Fc(0, 0, z_m) = \int_{\Re} Q_C(x, y) f(x, y) \mathrm{d}x\mathrm{d}y \tag{1}$$

where $\Re$ denotes the integration domain (0 to ∞), and *x*, *y* are the space coordinates. We used two well-performing analytical models to interpret the turbulent transport of carbon fluxes generated from the heterogeneous surface. These include:

1) Korman and Meixner approach (KM Model): This method provides an analytical solution to the two-dimensional advection–diffusion equation by considering power-law profiles for horizontal wind velocity (*u*) and eddy diffusivity (*K*) (Kormann and Meixner 2001). The two profiles are further related to Monin–Obukhov similarity profiles using an analytical (Huang et al. 1979) or a numerical root-finding approach. The analytical approach is adopted in this study to consider stationary flow conditions over homogeneous, isotropic terrains and to estimate cross-wind integrated fluxes at a downstream distance ($x > 0$), as given by:

$$f(x) = \frac{1}{\Gamma(\mu)} \frac{\xi^\mu}{x^{1+\mu}} e^{\left(-\frac{\xi}{x}\right)} \tag{2}$$

where, $\Gamma(x)$ is the Gamma function, μ is a parameter that depends on atmospheric stability conditions, and $\xi(z)$ is the length scale parameter. Among the available analytical models, KM is the most preferred one due to realistic profiles of 'u' and 'K', applicability over a wide range of stability conditions, and numerical stability. Although KM model gives an approximate solution, the method uses atmospheric stability parameters as input instead of surface roughness parameters.

2) Flux footprint prediction approach (FFP): This method provides an analytical solution to the Lagrangian model, with an application to a wide range of boundary layer conditions and measurement heights (Xu et al. 2019). The two-dimensional footprint function is expressed in terms of crosswind-integrated footprint $\overline{f^y}$ and a crosswind dispersion function Dy (Horst and Weil 1992) given by:

$$D_y(x, y) = \frac{e^{\frac{-y^2}{2\sigma_y^2}}}{\sqrt{2\pi}\sigma_y} \tag{3}$$

where x, y are the space coordinates and σ_y is expressed as a function of atmospheric stability and distance downwind of the source (Horst and Weil. 1992)

$$f(x, y) = \overline{f^y}(x) D_y \tag{4}$$

The method uses a scaling approach and parameterization to estimate $\overline{f^y}$ and lateral dispersion (D_y) from turbulent parameters, thereby eliminating long computational times associated with the release of a large number of trajectories. The model simulates a continuous range of stabilities from stable to convective while satisfying the well-mixed condition of Thomson (1987) everywhere. FFP requires stationarity and horizontal homogeneity of the flow over time periods and its simulations are limited to measurement heights above the roughness sublayer and below the entrainment layer.

2.3.2 Averaging surface characteristics

Despite refinement, there has been limited application of analytical models to heterogeneous landscapes as the changing surface characteristics (such as topography, roughness length, leaf area) are not considered. This makes it difficult to interpret experimental footprints using model parameters obtained for homogeneous surfaces. Hence, we modified roughness length used in analytical models to suit changed roughness conditions through parameter aggregation.

2.3.2.1 Parameter aggregation (arithmetic average) This method employs simple arithmetic mean of input param-

eters (e.g., aerodynamic roughness length) from contributing parcels in estimating fluxes.

$$\overline{z_{arith}} = \frac{1}{N} \sum_{i=1}^{N} z_{oi} \tag{5}$$

where, $\overline{z_{arith}}$ is average roughness length used in footprint computations, z_{oi} is roughness length from the surface 'i' out of 'n' surfaces. Oversimplification of underlying physics makes this a less preferred method, particularly in regions with strong turbulence and contrasting surface characteristics (Göckede et al. 2006).

2.3.2.2 Parameter aggregation (area-weighted average) This method employs area-weighted mean of input parameters (e.g.: aerodynamic roughness length) from contributing parcels in estimating heterogeneous fluxes.

$$\overline{z_{area}} = \frac{1}{A} \sum_{i=1}^{N} A_i * z_{oi} \tag{6}$$

where $\frac{A_1}{A}, \frac{A_2}{A}, \dots . \frac{A_n}{A}$ are areal proportions of individual homogeneous surfaces within the footprint of high tower.

2.3.2.3 Effective input parameters Previously discussed averaging methods disregard non-linearity between surface characteristics and contributing fluxes. As a result, use of simple or weighted average parameters may result in altogether different flow characteristics that represent neither of the underlying surfaces. This method uses a logarithmic average of roughness length normalized with friction velocity to represent effective roughness length (Foken and Leclerc 2004; Hasager and Jensen 1999; Taylor 1987).

$$\overline{z_{eff}} = \frac{\overline{u_* . \ln z_o}}{\overline{u_*}} \tag{7}$$

where z_o is the roughness length, $u*$ is the frictional velocity, and z_{eff} is the aggregate roughness length. Since KM model indirectly considers roughness length (via $U/u*$) as an input, we matched the calculated roughness length with aggregated parameter value prior to footprint prediction. A R code is developed to estimate flux footprint using KM method. Since FFP directly considers roughness length as input parameter, we used the online tool developed by Kljun et al. (2015) (https://geography.swansea.ac.uk/nkljun/ffp) to implement parameter aggregation. A time series of input data is uploaded in prescribed format in the FFP online tool. Footprints are estimated for each time step, and aggregated to a footprint climatology. The online tool provides 1D as well as 2D flux footprints from the input parameters observed by the flux tower. While FFP-1D tool provides the

crosswind integrated flux footprint, FFP-2D uses time-series of input datasets and provides footprint climatology along with underlying unsupervised classified land cover. The tool overlays land cover classes on footprint climatology to provide an estimate of which land cover contributes most to the measured fluxes (Kljun et al. 2015).

2.4 Sobol sensitivity analysis

To better understand the contribution of each input parameter (as well as their interactions) on simulated fluxes under heterogeneous conditions, we performed variance-based Sobol sensitivity analysis (Zhang et al. 2015). This method allows for the identification of a parameter (or set of parameters) with the most significant influence on output variance. Input parameters considered include: upwind distance (x), wind velocity (U), Obukhov length (L), friction velocity (u^*), and roughness length (z_0). These parameters were varied over a finite range and rescaled to [0, 1]. Carbon fluxes were assessed as a function of the input parameter set using a Monte Carlo approach following probabilistic interpretation. This method decomposes output variance into a sum of variances of input parameters in increasing dimensionality to determine contributions of each input parameter and their interactions to overall variance. Algorithm outputs include: first-order (contribution of a single parameter), second-order (contribution of parameter interactions), and total-order (combination of main and higher-order effects) sensitivity indices. The main effects or first-order sensitivity indices measure the fractional contribution of a single parameter to the output variance whereas, second-order sensitivity indices are used to measure the fractional contribution of parameter interactions to the output variance. The total order sensitivity indices consider both main, second-order, and higher-order effects which involve the evaluation over a full range of parameter space (SOBOL' 1993). As the order of sensitivity indices increases, the model parameters and associated steps become more influential. An arbitrary threshold of 0.1 is considered to differentiate important and unimportant parameters. A comprehensive discussion on Sobol's sensitivity analysis and its implementation can be found in Zhang et al. (2015).

2.5 Flux contribution from individual land use

Parameter aggregation methods are designed to estimate fluxes in a mixed fetch environment by modifying input parameters. However, these methods do not estimate proportional contributions of individual landmasses. Flux partitioning overcomes this limitation using the principle of superposition (Arriga et al. 2017; Foken and Leclerc 2004; Leclerc and Foken 2014a). In brief, the combined fluxes measured by the high-tower (F_{T3}) is considered as the weighted sum of

fluxes measured by the two low-height towers (that capture homogenous fluxes: F_{T1} and F_{T2}) given by:

$$F_{T3} = \alpha * F_{T1} + \beta * F_{T2} + E \tag{8}$$

where α and β (range 0–1) are proportional contributions of fluxes generated from sugarcane and cotton fields, respectively. The 'noise' term (E) represents 'closing error' containing the fluxes generated from outside the field boundaries as well as interaction fluxes. The optimal values of α and β that satisfy Eq. (8) were obtained using least square minimization. Proportional contributions depend on a number of surface and atmospheric characteristics including roughness length $\left(z_0\right)$, atmospheric stability $\left(\frac{z-d}{L}\right)$, source areas ($\frac{A_1}{A}$ and $\frac{A_2}{A}$), wind velocity (U), and friction velocity (u^*).

2.6 Performance evaluation

We used four goodness-of-fit indicators to evaluate performance of parameter-aggregated analytical models in simulating flux footprints under heterogeneous conditions. These include: (i) coefficient of determination (R^2), (ii) root mean square error (RMSE), (iii) bias of estimation (PBIAS), and (iv) modelling efficiency (NSE). These indicators were computed from the pairs of EC observed (O_i) and analytical model simulated (P_i) fluxes, as well as their means ($\overline{O,P}$) for various upwind distances. Coefficient of determination (R^2) provides the strength of linear relation between observed and model estimated fluxes. Root mean squared error (RMSE) measures the variance of residual errors. Percentage bias (PBIAS) indicates the average tendency of the simulated data to be larger or smaller than the corresponding observations made at the high tower (T3). Similarly, Nash–Sutcliffe efficiency (NSE), determines the relative magnitude of the residual variance compared to the measured data variance. We judged the model ability to estimate flux footprints over heterogeneous surfaces to result in a high R^2 and NSE (that would ideally approach 1), minimum RMSE, and PBIAS (that would ideally approach 0).

3 Results and discussion

This section provides a detailed analysis of fluxes generated from heterogeneous croplands with varying surface roughness lengths. As footprint models rest on the assumptions of profiles of turbulence parameters, we first analysed the diurnal cycles of atmospheric and turbulence parameters as monitored by the high tower. This will also help to apply similarity theories, which is the basis for footprint prediction using analytical models. EC fluxes generated from two distinct surfaces resulting from progressive harvesting (experiment 1) were used to

evaluate and improve the performance of the analytical models (KM and FFP) with modified surface roughness (z_0) inputs. Knowing the importance of turbulence characteristics over surface roughness on estimated footprints, we then analysed the contribution of individual surfaces (experiment 2) to the fluxes measured in a heterogenous cropland under changing turbulent regimes.

3.1 Turbulent conditions

As the two-crop surface experiment has lasted for a longer period, diurnal cycles of turbulent parameters during this period (01 Apr–9 Dec, 2018, i.e. DOY: 91–353, 2018) for the high tower (T3) were analyzed and presented in Fig. 3. Variation in turbulent parameters has three distinct time-windows within which the values are fairly constant. These include: (i) early hours, i.e. 00:00 to 08:00, (ii) daylight hours, i.e. 10:00 to 16:00, and (iii) nocturnal hours, i.e.
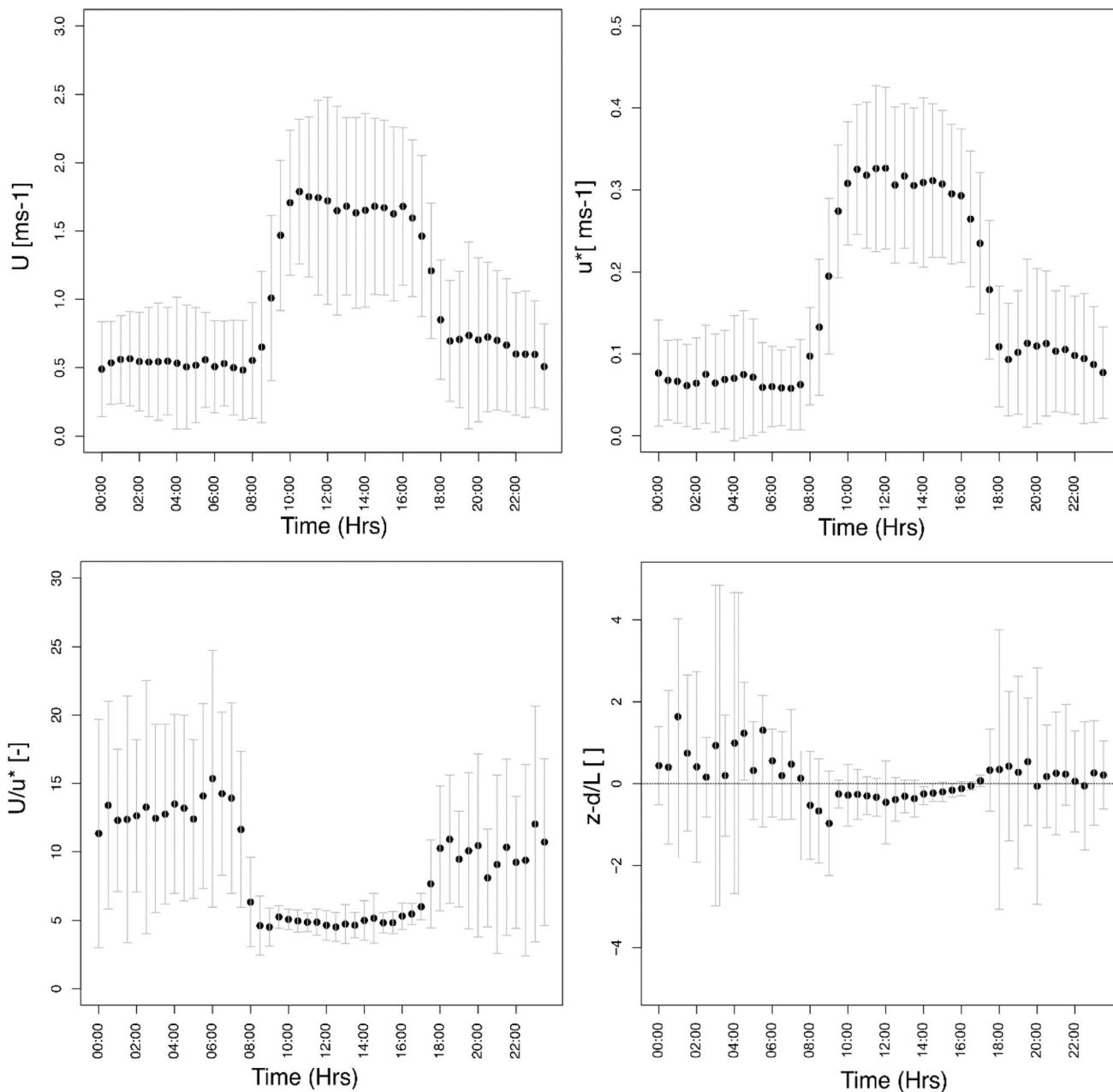
Fig. 3 Diurnal variations showing mean and one standard deviation of: **a** wind velocity (*U*), **b** friction velocity (*u**), **c** *U/u**, and **d** stability parameter (*z − d/L*) observed at *T*3 during the monitoring period (01 Apr–19 Dec, 2018, i.e. DOY: 91–353, 2018)

18:00 to 00:00. Both wind speed (U) and friction velocity (u^*) showed a similar trend with low magnitudes during early hours (0.52 ± 0.02 ms^{-1}; 0.06 ± 0.00 ms^{-1}), sustained peak during daylight hours (1.67 ± 0.07 ms^{-1}; 0.30 ± 0.01 ms^{-1}), and returned to low magnitudes during nocturnal hours (0.71 ± 0.17 ms^{-1}; 0.10 ± 0.02 ms^{-1}). The ratio: $\frac{U}{u^*}$ (being proxy for surface roughness, z_o (Arriga et al. 2017)) varied significantly throughout the monitoring period (8.99 ± 2.86) and followed an opposite trend to variation in U. The variation in $\frac{U}{u^*}$ was almost similar for the three towers, suggesting that any change in friction results in an equivalent change in mean flow, thus making fluxes less dependent on roughness changes. A steep change in these variables during 08:00 to 10:00 and 16:00 to 18:00 Hrs time-windows is responsible for changes in atmospheric stability and eddy circulation. Highly unstable atmospheric conditions were prevailed during daylight hours ($\frac{z-d}{L}$: -0.45 ± 0.585) and are weakly correlated with U and u^* ($R^2 < 0.1$). A smooth transition from stable to neutral and then to unstable atmospheric conditions was observed from 06:00 to 10:00 Hrs. Even though low wind speeds and small eddy formation during stable atmospheric conditions facilitate flux measurement, increased fetch from multiple landscapes makes interpretation cumbersome. Enhanced convection and turbulent diffusion during unstable atmospheric conditions have resulted in a smaller source area, favourable for experimentation. Thus, we restricted data monitoring to daylight hours (10:00 to 18:00) so that only two surfaces will contribute to the fluxes observed by the high tower. Wind direction throughout the day time was fairly constant ($\sim 45° \pm 12°$ from the North). We observed a significant change in wind direction from East to North–East after 08:00 Hrs. All towers were aligned at 90° from the North to minimize the effects of cross currents. The standard deviation of lateral wind speed (σ_v) was found to be about one-fourth of mean longitudinal wind ($\overline{U}$). Biases in fluxes caused by changes in mean wind direction were negligible (Kumari et al. 2020) and are not considered further. Over the course of the study period, and for unstable atmospheric conditions, sensible heat, H (Wm^{-2}) was varied between 138.99 ± 34.95, latent heat, LE (Wm^{-2}) between 109.63 ± 42.41, Obukhov length (m) between (28.62 ± 31.44), and friction velocity (ms^{-1}) between 0.32 ± 0.07. The strength of the linear association between available energy (Rn–G) and turbulent fluxes (H+LE) is 0.96, confirming a good energy balance closure.

3.2 Performance of footprint models under changing roughness conditions

For the same atmospheric and surface conditions, there can be obvious differences in the behaviour of footprint models (Hui and Xuefa 2015; Kljun et al. 2015; Arriga et al. 2017; Heidbach et al. 2017; Prajapati and Santos 2017; Kumari et al. 2020). Successive cut experiment has resulted in multiple source area envelopes resulting from different roughness lengths. Figure 4 shows the model-derived footprints for a reference mast height (Z_m) of 8 m, with varying roughness lengths (Eqs. 4–6). A total of five roughness lengths specific to: homogeneous cut surface, z_1; homogeneous sugarcane, z_2; arithmetic average, z_3; area weighted average, z_4; and effective roughness length, z_5 were used in an ensemble mode. Parameters
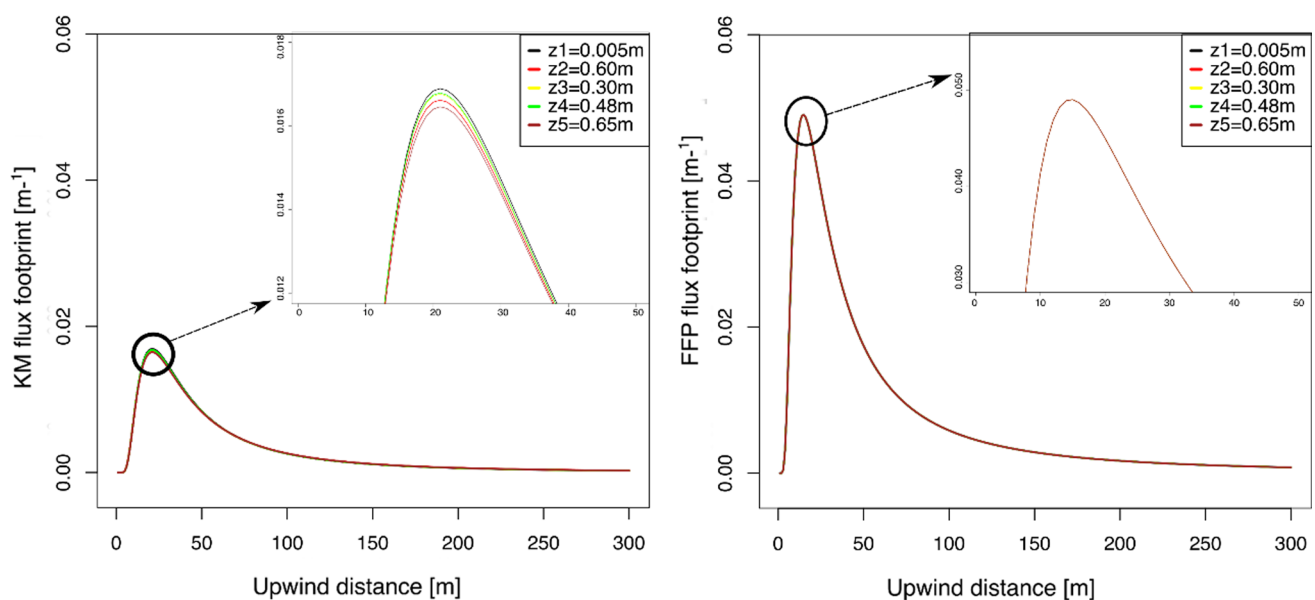

Fig. 4 Cross-wind integrated flux footprints, using **a** KM model and **b** FFP model considering modified roughness length parameters ($z1$ thru $z5$) under unstable atmospheric conditions ($U = 2.51$ ms^{-1}, $u^* = 0.29$ ms^{-1}, and $(z-d)/L = -0.09$)

used in the model development include: $U = 2.51$ ms^{-1}, $u* = 0.29$ ms^{-1}, and $(z{-}d)/L = -0.09$. While FFP considers roughness length as a direct input, the KM model indirectly considers roughness length via U/$u*$ values. Model footprints for given conditions are characterized by a single-peaked curve with a steep rising limb (slope: 18.8×10^{-3} with KM, 0.0138 with FFP), followed by a gentle recession (slope: 3×10^{-4} with KM, 2.3×10^{-4} with FFP). The contribution of surface fluxes was significant up to a distance of about 150 m (levelling off in Fig. 4), which is falling outside the boundary of the sugarcane field (Fig. 2). As the neighbouring fields are mowed, contribution of fluxes generated outside the sugarcane field is considered to be negligible. In comparison to FFP, the KM model has underestimated and delayed the footprint peak. We observed little to no improvement in footprint representation between the scenarios, perhaps due to a small deviation in average roughness length values considered (0.30–0.65 m) from that of sugarcane (0.60 m) or cut surface (0.005 m). The similarities in roughness between our target land classes are unlike the abrupt changes observed by Heidbach et al. (2017) between grasslands and forests.

Data from successive cut experiment was further utilized to evaluate the performance of two footprint models under changing surface roughness and source area conditions (Arriga et al. 2017). For this, we assumed only sugarcane and mowed surface will contribute to the fluxes measured by the high tower (forcing the closing error, E in Eq. 8 to zero). Contribution of sugarcane (α) and cut ($1 - \alpha$) surfaces to the fluxes monitored by the high-tower can be estimated from:

$$F_{T3} = \alpha \cdot F_{T1} + (1 - \alpha) \cdot F_{T2} \tag{9}$$

with, F_{T1}, F_{T2}, and F_{T3} representing the carbon fluxes measured by the three towers T1, T2, and T3. During the experiment, α was gradually decreased from 0.8 (cut-1) to 0.0 (cut-5), and the corresponding cumulative footprints as a function of distance are plotted in Fig. 5. Error bars represent the contribution of sugarcane surface to the measured fluxes during each of the five cuts. With a reduction in crop stretch and extension of dragging canopy, the estimated z_0 values were decreased resulting in a slight expansion of footprint (Leclerc and Foken 2014a, b; Rannik et al. 2012). As the aerial contribution of individual surfaces changes during each cut, a discontinuous footprint model was observed with the area-weighted roughness ($z4$) model. KM model performance was gradually changed from over prediction at lower source area (α) contribution to under prediction at higher source area contributions. Whereas FFP model has consistently over-predicted the source area contributions due to inherent representation of landscape heterogeneity during footprint estimation. As the contribution of nearby fields to the high tower (T3) fluxes increases, which is indicated by lowering of α, FFP model results are in congruence with experimentally obtained cut fractions. On the contrary, when only sugarcane field is contributing to the high tower fluxes (indicated by a high α), the KM model performed better. This concludes that, applicability of the KM model in heterogeneous conditions is relatively poor. The cumulative footprints predicted by the two models were levelled off after about 150 m, which is beyond the boundary of the sugarcane
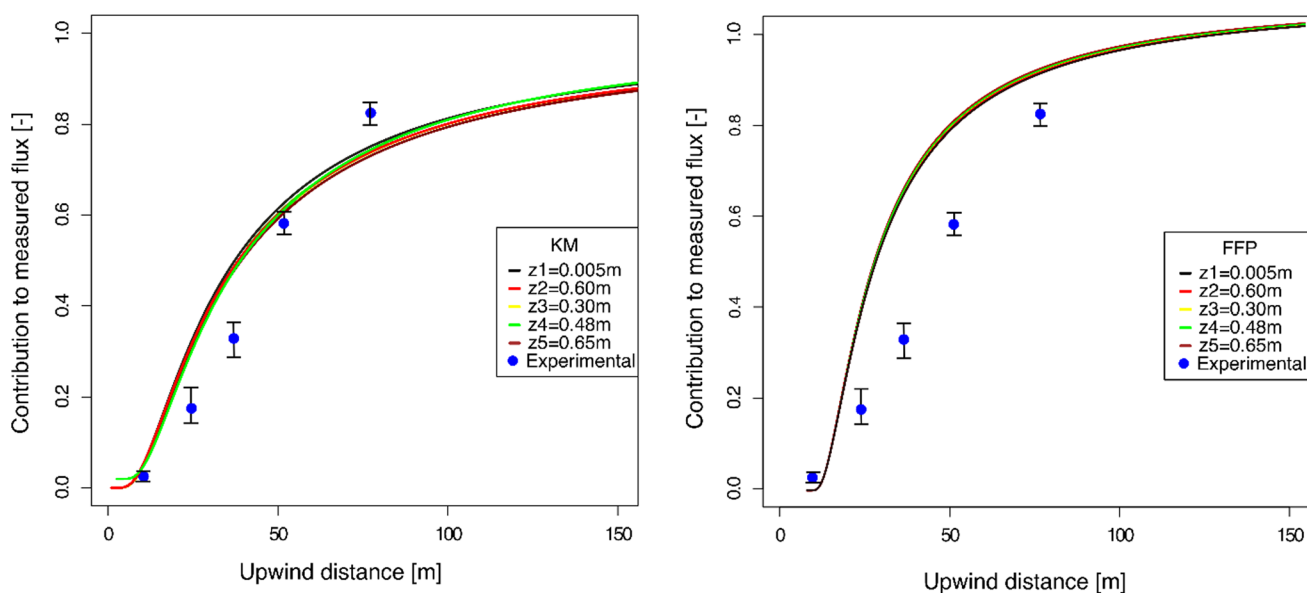

Fig. 5 Cumulative flux contributions using **a** KM model, and **b** FFP model for different cuts ($x = 10$ m, 25 m, 40 m, 55 m, and 80 m) considering modified roughness parameters in unstable atmospheric conditions ($U = 8.42$ ms^{-1}, $u* = 0.29$ ms^{-1}, and $(z - d)/L = -0.09$). Error bars represent the observed flux contribution for different upwind distances from T3

surface. Since the nearby fields were mowed, contribution of fluxes from outside the sugarcane field is negligible.

The vertical offsets between measured and simulated 'α' contributions for all upwind distances were further used to evaluate parameter aggregation techniques (Table 1). With a sample size (n) of 1,171, FFP model resulted in RMSE of 0.31, MBE of -0.08, NSE of 0.25, and PBIAS of 19.0. Similarly, KM model resulted in RMSE of 0.02, MBE of 0.03, NSE of 0.06–0.07, and PBIAS of 8.50–8.90. RMSE and MBE were close to zero owing to low 'error' magnitudes. Both models are biased to the lower side of experimental data and statistical parameters were similar irrespective of the averaging method used for roughness length. We conclude that parameter aggregation could not improve the performance of footprint models (under changing source area) due to negligible variation in roughness length across the surface.

3.3 Sensitivity of footprint models

Knowing the fact that roughness length changes have a trivial effect, we performed global sensitivity analysis to better understand the role of surface-layer forcing on footprint predictions (Sobol algorithm; (SOBOL' 1993). The method uses a Monte Carlo approach to decompose the variance in model outputs into proportions attributed to sets of inputs. The algorithm to estimate Sobol indices for first-order and total-order was developed in open-source 'R' using 'Sensitivity' package (https://CRAN.R-project.org/package=sensitivity) with a total computational cost of $(p+2) \times n$ model evaluations (where, p is the number of factors and n is the sample size). We tested sensitivities of the two models (KM and FFP) to five input parameters, i.e., upwind distance (x), mean wind speed (U), Obukhov length (L), friction velocity (u^*), and roughness length (zo). Parameter ranges considered in the analysis are as follows: $x-0$ to 100 m, $U-0.082$ to 2.79 ms^{-1}, $L-1.03$ to -116.53 m, $u^*-0.03$ to 0.68 ms^{-1},

and zo -0.005 to 0.65 m. Input data were normalized with respective maximum values for ease with comparison. We used a sample size of 10,000 with uniform distribution of all input parameters. Results of Sobol sensitivity analysis with output sensitivities are shown in Fig. 6. As a whole, model derived footprints are sensitive to turbulent characteristics (U, and u^*), atmospheric stability (L), upwind distance (x), and showed a weak sensitivity to roughness parameters ($z0$). Footprint predictions using KM model are more sensitive to upwind distance, atmospheric stability, and wind speed, while friction velocity and roughness length have a negligible impact. Considering the FFP model, footprint predictions are sensitive to upwind distance, wind speed, and friction velocity. Changes in surface roughness and atmospheric stability had a little impact on model footprints. Except for U and u^*, the two models have responded similarly to input parameters. This motivated us to analyse heterogenous fluxes under changing turbulent conditions (U, u^*) rather than surface roughness ($z0$), resulting in experiment-2. A high dependence of upwind distance (x) on model footprints confirm that the measured fluxes are influenced by heterogeneity. Analytical models mainly consider x, U, and u^* in flux footprint estimation. As these are not varied during parameter averaging, they did not contribute to model improvement. Our findings support those of Arriga et al. (2017) and Kumari et al. (2020). Of the two models, FFP performed slightly better, owing to a better interpretation of changes in roughness length during flux estimates.

3.4 Flux partition in heterogeneous conditions

The difference in sensitivities between the two models clearly highlight the difference in methodological approaches to estimate the footprints. In order to ensure the maximum flux contribution from the two surfaces, i.e. sugarcane and cotton, isopleths of varying intensities were considered. Footprint climatology showing two-dimensional

Table 1 Residual statistical parameters used in the comparison of parameter aggregation methods in estimating flux footprints from inhomogeneous landscapes

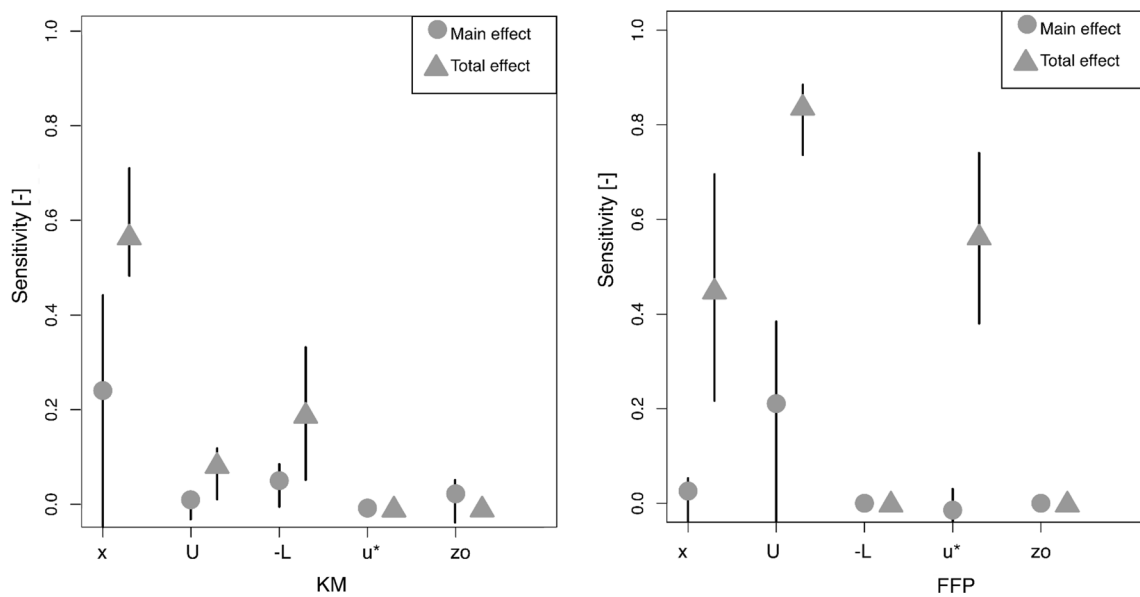| *FFP model*					
Method	zo [m]	RMSE [–]	PBIAS [–]	NSE [–]	R^2 [–]
Arithmetic average	0.30	0.31	19.00	0.25	0.49
Area weighted average	0.48	0.31	19.00	0.25	0.49
Effective input parameter	0.65	0.31	19.00	0.25	0.49
KM model					
Method	zo [m]	RMSE [–]	PBIAS [–]	NSE [–]	R^2 [–]
Arithmetic average	0.30	0.02	8.50	0.06	0.68
Area weighted average	0.48	0.02	8.60	0.06	0.68
Effective input parameter	0.65	0.02	8.90	0.07	0.68

Fig. 6 Sensitivity of roughness and turbulence parameters on footprint predictions using KM (left) and FFP (right) models. Effect of variation in individual parameters (main effect) as well as its interaction with other parameters (total effect) was computed using the Sobol algorithm

Fig. 7 Footprint climatology showing two-dimensional source area of flux measurements from the three towers under unstable stratification. Isopleths of different percentage contributions to the total flux are indicated with solid lines. Tower positions are indicated by a plus mark

isopleths of different source area contributions superimposed on land use map is presented in Fig. 7. We used two-dimensional FFP online tool (Kljun et al. 2015) to generate an ensemble of footprints considering multiple time steps during unstable atmospheric conditions. Isopleths of X % ($0 \leq X \leq 100$) represent the area contributing to X % of the total measured flux, such that all the cells lying within the X-isopleth have each accumulated flux contributions of up to X % of the measured fluxes. Isopleths beyond 90% threshold were not displayed as they correspond to much larger areas. These figures reveal that, for up to 80% isopleths, both T1 and T2 are capturing fluxes originating from the individual sugarcane and cotton fields, respectively. Similarly, for the high-tower T3, the contribution of the two fields alone to the measured fluxes is significant beyond 70% and up to 80% isopleths. Also, most parts of the 70–80% isopleths have recorded good quality of the carbon fluxes (classes: 0 and 1). Hence, we have considered the fluxes within 80% isopleth (that captures the fluxes mostly from the cotton and sugarcane fields during unstable conditions) to minimize the disturbances caused by the effect of neighbouring fields. Availability of only three EC towers has restricted our application to two crop surfaces and to neglect the contribution of fluxes from other fields.

As the effect of turbulence on footprint estimates is significant and dynamic, we analyzed the diurnal fluxes monitored by the three towers within the 80% isopleth under unstable atmospheric conditions. Variations in daytime carbon exchanges were assessed across four-time steps: (i) 10:00 to 12:00; (ii) 12:30 to 14:00; (iii) 14:30 to 16:00; and (iv) 16:30 to 18:00. Variation in $u*$ for these four time steps are, respectively: 0.15 to 1.16 ms^{-1}, 0.14 to 1.12 ms^{-1}, 0.11 to 0.98 ms^{-1}, and 0.0316 to1.06 ms^{-1}. Obukhov length (L) gradually declined (e.g., from -1.03 m at 10:00 Hrs to -116.53 m at 16:30 Hrs) as the day progressed. Contribution of fluxes from sugarcane (α) and cotton (β) fields to the high tower (T3) observations during different hours of the day is shown in Fig. 8. Optimal values of α and β for given turbulence characteristics were obtained by regressing mixed fluxes against a linear combination of homogeneous fluxes using 'lm function' in RStudio (V. 3.6.2). Both α and β were fairly constant throughout the day ($\alpha \sim 0.25$, $\beta \sim 0.45$), with an exception during 14:30 to 16:00 Hrs ($\alpha \sim 0.45$, $\beta \sim 0.2$). A sudden increase in the flux contribution from Cotton field around 14:30 to 16:00 Hrs is observed resulting from the sudden transition in wind speed, turbulent characteristics (U, $u*$) and atmospheric stability ($z - d/L$). We note that the sum of error and interaction terms ($1 - (\alpha + \beta)$) were significant throughout the day (> 0.2).

The contribution of individual fields to the mixed fluxes within the 70–90% isopleths of the high-tower, averaged over
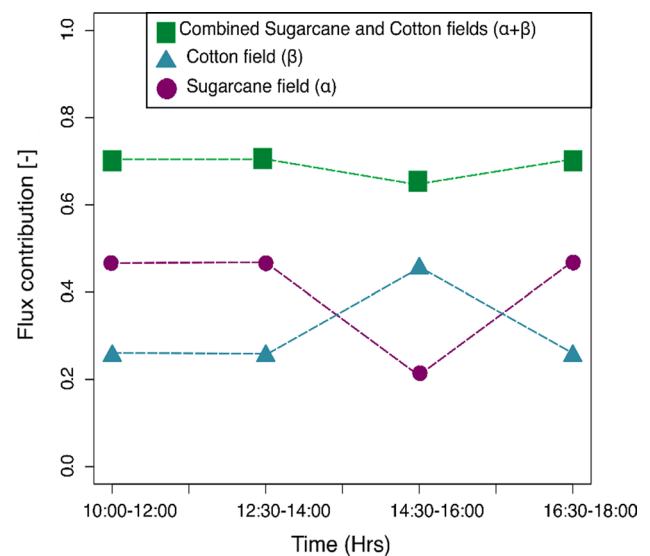

Fig. 8 Diurnal variations in the contribution of sugarcane (α) and cotton (β) fields to the heterogeneous fluxes under unstable atmospheric conditions

the day are presented in Fig. 9. The contribution of sugarcane field (α) was progressively declined from 70% to 55% as the isopleth purview was enhanced from 70% to 90%. During this enhancement, there was a complementary increase in fluxes generated from the surrounding fields (from 5% to 25%). At 70% isopleth, both sugarcane (α) and cotton (β) fields were collectively contributing to 90% of the observed fluxes, which was decreased to 78% at 90% isopleth. This concludes that the contribution of both sugarcane and cotton fields decreases towards higher isopleths with a higher rate for sugarcane than for cotton.

Validation of footprint models of varying complexity with experimental data as in Fig. 5 has improved our understanding of footprint representation over complex heterogeneous surfaces. Findings of this study can help in extending footprint models to other heterogeneous surfaces and bifurcate the fluxes measured by EC tower in mixed-fetch conditions. In a broader sense, the outcome of this study can help to: (i) characterize water use efficiency (ratio of carbon to water fluxes) in fragmented crop lands, (ii) understand carbon and methane exchanges between atmosphere and cropland ecosystem. Availability of only three EC towers has restricted our application to two crop surfaces and to neglect the contribution of fluxes from other areas. We considered only 80% of the total fluxes observed by EC system so as to neglect the contribution of fluxes from the nearby fields. The modelled and measured flux footprint estimates are site and setup specific.

Fig. 9 Frequency distribution of relative contributions of sugarcane and cotton fields to total fluxes for different isopleths, under daytime unstable measurements ($u^* = 0.0316$ to 1.166 ms^{-1}, $L = -1.03$ m to -86.53 m)
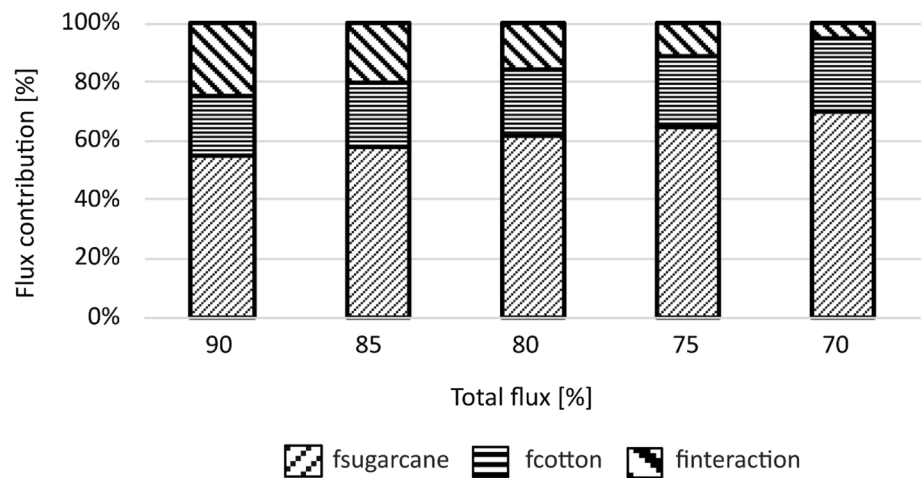
4 Conclusion

This study presents an experiment-based flux footprint analysis in fragmented heterogeneous cropland system. Two flux monitoring experiments using three EC towers were performed in fragmented croplands characterised by contrasting surfaces with objectives to: (i) quantify the heterogeneous fluxes using two footprint models (KM and FFP) with modified roughness parameters and (ii) bifurcate the fluxes into contributing homogenous fluxes using the principle of superposition. The main observations of the study are as follows:

1. The first objective was achieved by a successive cut experiment on a homogeneous sugarcane field, and apply KM and FFP models with varying roughness length parameters to represent changes in source area contributions, as measured by the high-tower. FFP model has consistently overestimated the footprints, KM model predictions are found to be a function of upwind distance.

2. Parameter aggregation methods failed to incorporate the heterogeneity of canopy surface using surface roughness length as we observed little to no improvement in model footprints due to marginal changes in roughness length. Parameter aggregation methods thus need to be revisited to consider the effect of smaller variations in roughness length.

3. Sensitivity analysis revealed that KM and FFP model footprint prediction are more sensitive to meteorological conditions (U, u^*, L) and upwind distance (x), than to roughness length (zo).

4. The second objective is achieved by monitoring fluxes in a sugarcane–cotton field setup under varying turbulent conditions throughout the day hours. A drastic decrease in sugarcane field flux contribution happened between 14:30 and 16:00 Hrs contrary, the contribution of cotton field increased. The change in contribution to the measured fluxes happened with the change in atmospheric stability ($z - d/L$), wind speed, turbulence characteristics (U, u^*).

5. Contribution of fluxes generated from nearby fields was found to be significant at higher isopleths (> 80%) which requires a careful attention while designing flux footprint studies.

6. The modelled and measured flux footprints are site specific as well as setup specific and stable stratification is not considered in the study. The heterogeneity in the sites can be due to topography also but heterogeneity originating from canopy surface is only considered in the study.

This work can be further extended to heterogenous canopy with varying management conditions and help in improving flux-based water use management strategies in fragmented croplands.

References

Arriga N, Rannik Ü, Aubinet M, Carrara A, Vesala T, Papale D (2017) Experimental validation of footprint models for eddy covariance CO2 flux measurements above grassland by means of natural and artificial tracers. Agric for Meteorol 242:75–84. https://doi.org/10.1016/j.agrformet.2017.04.006

Aubinet M, Grelle A, Ibrom A, Rannik Ü, Moncrieff J, Foken T et al (1999) Estimates of the annual net carbon and water exchange of forests: the EUROFLUX methodology. Adv Ecol Res 30:113–175

Avissar R, Pielke RA (1989) A parameterization of heterogeneous land surfaces for atmospheric numerical models and its impact on regional meteorology. Mon Weather Rev 117:2113–2136

Beyrich F, Leps J-P, Mauder M, Bange J, Foken T, Huneke S et al (2006) Area-averaged surface fluxes over the LITFASS region based on eddy-covariance measurements. Bound-Layer Meteorol 121(1):33–65. https://doi.org/10.1007/s10546-006-9052-x

Chu H, Luo X, Ouyang Z, Chan WS, Dengel S, Biraud SC et al (2021) Representativeness of eddy-covariance flux footprints for areas surrounding AmeriFlux sites. Agric for Meteorol 301–302:108350. https://doi.org/10.1016/j.agrformet.2021.108350

Feigenwinter C, Vogt R, Christen A (2012) Eddy covariance measurements over urban areas. In: Aubinet M, Vesala T, Papale D (eds) Eddy covariance: a practical guide to measurement and data analysis. Springer Netherlands, Dordrecht, pp 377–397. https://doi.org/10.1007/978-94-007-2351-1_16

Foken T, Leclerc MY (2004) Methods and limitations in validation of footprint models. Agric for Meteorol 127(3):223–234. https://doi.org/10.1016/j.agrformet.2004.07.015

Foken T, Wichura B (1996) Tools for quality assessment of surface-based flux measurements. Agric for Meteorol 78(1):83–105. https://doi.org/10.1016/0168-1923(95)02248-1

Foken T, Göockede M, Mauder M et al (2005) Post-field data quality control. In: Lee X, Massman W, Law B (eds) Handbook of micrometeorology. Kluwer Academic Publishers, Dordrecht, pp 181–208

Göckede M, Rebmann C, Foken T (2004) A combination of quality assessment tools for eddy covariance measurements with footprint modelling for the characterisation of complex sites. Agric for Meteorol 127(3):175–188. https://doi.org/10.1016/j.agrformet.2004.07.012

Göckede M, Markkanen T, Mauder M, Arnold K, Leps J-P, Foken T (2005) Validation of footprint models using natural tracer measurements from a field experiment. Agric for Meteorol 135(1):314–325. https://doi.org/10.1016/j.agrformet.2005.12.008

Göckede M, Markkanen T, Hasager CB, Foken T (2006) Update of a footprint-based approach for the characterisation of complex measurement sites. Bound-Layer Meteorol 118(3):635–655. https://doi.org/10.1007/s10546-005-6435-3

Göckede M, Foken T, Aubinet M et al (2008) Quality control of CarboEurope flux data – Part 1: Coupling footprint analyses with flux data quality assessment to evaluate sites in forest ecosystems. Biogeosciences 5:433–450. https://doi.org/10.5194/bg-5-433-2008

Hasager CB, Jensen NO (1999) Surface-flux aggregation in heterogeneous terrain. Q J R Meteorol Soc 125(558):2075–2102. https://doi.org/10.1002/qj.49712555808

Heidbach K, Schmid HP, Mauder M (2017) Experimental evaluation of flux footprint models. Agric for Meteorol 246:142–153. https://doi.org/10.1016/j.agrformet.2017.06.008

Horst TW (1999) The footprint for estimation of atmosphere-surface exchange fluxes by profile techniques. Bound-Layer Meteorol 90(2):171–188. https://doi.org/10.1023/A:1001774726067

Horst TW, Weil JC (1992) Footprint estimation for scalar flux measurements in the atmospheric surface layer. Bound-Layer Meteorol 59(3):279–296. https://doi.org/10.1007/BF00119817

Horst TW, Weil JC (1994) How far is far enough? The Fetch requirements for micrometeorological measurement of surface fluxes. J Atmos Ocean Technol 11(4):1018–1025. https://doi.org/10.1175/1520-0426(1994)011%3c1018:HFIFET%3e2.0.CO;2

Hsieh C-I, Katul G, Chi T (2000) An approximate analytical model for footprint estimation of scalar fluxes in thermally stratified atmospheric flows. Adv Water Resour 23(7):765–772. https://doi.org/10.1016/S0309-1708(99)00042-1

Huang T, Yang G, Tang G (1979) A fast two-dimensional median filtering algorithm. IEEE Trans Acoust Speech Signal Process 27(1):13–18. https://doi.org/10.1109/TASSP.1979.1163188

Hui Z, Xuefa W (2015) Flux footprint climatology estimated by three analytical models over a subtropical coniferous plantation in Southeast China. J Meteorol Res 29(4):654–666

Kaharabata SK, Schuepp PH, Ogunjemiyo S, Shen S, Leclerc MY, Desjardins RL, MacPherson JI (1997) Footprint considerations in BOREAS. J Geophys Res Atmos 102(D24):29113–29124. https://doi.org/10.1029/97JD02559

Kljun N, Rotach MW, Schmid HP (2002) A three-dimensional backward Lagrangian footprint model for a wide range of boundary-layer stratifications. Bound-Layer Meteorol 103(2):205–226. https://doi.org/10.1023/A:1014556300021

Kljun N, Calanca P, Rotach MW, Schmid HP (2004) A simple parameterisation for flux footprint predictions. Bound-Layer Meteorol 112(3):503–523. https://doi.org/10.1023/B:BOUN.0000030653.71031.96

Kljun N, Calanca P, Rotach MW, Schmid HP (2015) A simple two-dimensional parameterisation for flux footprint prediction (FFP). Geosci Model Dev 8(11):3695–3713

Köppen W (1884) Die Wärmezonen der Erde, nach der Dauer der heissen, gemässigten und kalten Zeit und nach der Wirkung der Wärme auf die organische Welt betrachtet. Meteorologische Zeitschrift 1:5–226

Kormann R, Meixner FX (2001) An analytical footprint model for non-neutral stratification. Bound-Layer Meteorol 99(2):207–224. https://doi.org/10.1023/A:1018991015119

Kumari S, Kambhammettu BVNP, Niyogi D (2020) Sensitivity of analytical flux footprint models in diverse source-receptor configurations: a field experimental study. J Geophys Res Biogeosci 125(8):e2020JG005694. https://doi.org/10.1029/2020JG005694

Laurila T, Aurela M, Tuovinen J-P (2012) Eddy covariance measurements over wetlands. In: Aubinet M, Vesala T, Papale D (eds) Eddy covariance: a practical guide to measurement and data analysis. Springer Netherlands, Dordrecht, pp 345–364. https://doi.org/10.1007/978-94-007-2351-1_14

Leclerc MY, Foken T (2014a) Footprints in micrometeorology and ecology. Springer Berlin Heidelberg, Berlin. https://doi.org/10.1007/978-3-642-54545-0

Leclerc MY, Foken T (2014b) Practical applications of footprint techniques. In: Leclerc MY, Foken T (eds) Footprints in micrometeorology and ecology. Springer, Berlin, pp 199–224

Leclerc MY, Thurtell GW (1990) Footprint prediction of scalar fluxes using a Markovian analysis. Bound-Layer Meteorol 52(3):247–258. https://doi.org/10.1007/BF00122089

Leuning R (2007) The correct form of the Webb, Pearman and Leuning equation for eddy fluxes of trace gases in steady and non-steady state, horizontally homogeneous flows. Bound-Layer Meteorol 123(2):263–267. https://doi.org/10.1007/s10546-006-9138-5

Leuning R, Denmead OT, Lang ARG, Ohtaki E (1982) Effects of heat and water vapor transport on eddy covariance measurement of

CO2 fluxes. Bound-Layer Meteorol 23(2):209–222. https://doi.org/10.1007/BF00123298

Longdoz B, Granier A (2012) Eddy covariance measurements over forests. In: Aubinet M, Vesala T, Papale D (eds) Eddy covariance: a practical guide to measurement and data analysis. Springer Netherlands, Dordrecht, pp 309–318. https://doi.org/10.1007/978-94-007-2351-1_11

Markkanen T, Steinfeld G, Kljun N, Raasch S, Foken T (2009) Comparison of conventional Lagrangian stochastic footprint models against LES driven footprint estimates. Atmos Chem Phys 9(15):5575–5586. https://doi.org/10.5194/acp-9-5575-2009

Moureaux C, Ceschia E, Arriga N, Béziat P, Eugster W, Kutsch WL, Pattey E (2012) Eddy covariance measurements over crops. In: Aubinet M, Vesala T, Papale D (eds) Eddy covariance: a practical guide to measurement and data analysis. Springer Netherlands, Dordrecht, pp 319–331. https://doi.org/10.1007/978-94-007-2351-1_12

Optis M, Monahan A, Bosveld FC (2014) Moving beyond Monin-Obukhov similarity theory in modelling wind-speed profiles in the lower atmospheric boundary layer under stable stratification. Bound-Layer Meteorol 153(3):497–514. https://doi.org/10.1007/s10546-014-9953-z

Pasquill F, Smith FB (1983) Atmospheric diffusion: Study of the dispersion of windborne material from industrial and other sources

Prajapati P, Santos EA (2017) Measurements of methane emissions from a beef cattle feedlot using the eddy covariance technique. Agric for Meteorol 232:349–358. https://doi.org/10.1016/j.agrformet.2016.09.001

Rannik Ü, Sogachev A, Foken T, Göckede M, Kljun N, Leclerc MY, Vesala T (2012a) Footprint analysis. In: Aubinet M, Vesala T, Papale D (eds) Eddy covariance: a practical guide to measurement and data analysis. Springer Netherlands, Dordrecht, pp 211–261. https://doi.org/10.1007/978-94-007-2351-1_8

Rebmann C, Göckede M, Foken T, Aubinet M, Aurela M, Berbigier P et al (2005) Quality analysis applied on eddy covariance measurements at complex forest sites using footprint modelling. Theor Appl Climatol 80(2):121–141. https://doi.org/10.1007/s00704-004-0095-y

Schmid HP (1994) Source areas for scalars and scalar fluxes. Bound-Layer Meteorol 67(3):293–318. https://doi.org/10.1007/BF00713146

Schmid HP (1997) Experimental design for flux measurements: matching scales of observations and fluxes. Agric for Meteorol 87(2):179–200. https://doi.org/10.1016/S0168-1923(97)00011-7

Schmid HP (2002) Footprint modeling for vegetation atmosphere exchange studies: a review and perspective. Agric Forest Meteorol 113:159–183. https://doi.org/10.1016/S0168-1923(02)00107-7

Schmid HP, Oke TR (1990) A model to estimate the source area contributing to turbulent exchange in the surface layer over patchy terrain. Q J R Meteorol Soc 116(494):965–988. https://doi.org/10.1002/qj.49711649409

Schuepp PH, Leclerc MY, MacPherson JI, Desjardins RL (1990) Footprint prediction of scalar fluxes from analytical solutions of the diffusion equation. Bound-Layer Meteorol 50(1):355–373. https://doi.org/10.1007/BF00120530

Shweta07081992 (2022) Shweta07081992/Analysis-of-flux-footprints-in-fragmented-heterogeneous-croplands: analysis of flux footprints in fragmented, heterogeneous croplands. Zenodo. https://doi.org/10.5281/zenodo.6329725

SOBOL' IM (1993) Sensitivity analysis for non-linear mathematical models. Math Model Comput Exp 1:407–414

Stull R, Santoso E (2000) Convective transport theory and counter-difference fluxes. In: 14th symposium on boundary layer and turbulence, Aspen, CO, vol 7

Taylor PA (1987) Comments and further analysis on effective roughness lengths for use in numerical three-dimensional models. Bound-Layer Meteorol 39(4):403–418. https://doi.org/10.1007/BF00125144

Thomas C, Foken T (2002) Reevaluation of integral turbulence characteristics and their parameterisations

Thomson DJ (1987) Criteria for the selection of stochastic models of particle trajectories in turbulent flows. J Fluid Mech 180:529–556. https://doi.org/10.1017/S0022112087001940

Vesala T, Kljun N, Rannik Ü, Rinne J, Sogachev A, Markkanen T et al (2008) Flux and concentration footprint modelling: State of the art. Environ Pollut 152(3):653–666. https://doi.org/10.1016/j.envpol.2007.06.070

Vesala T, Eugster W, Ojala A (2012) Eddy covariance measurements over lakes. In: Aubinet M, Vesala T, Papale D (eds) Eddy covariance: a practical guide to measurement and data analysis. Springer Netherlands, Dordrecht, pp 365–376. https://doi.org/10.1007/978-94-007-2351-1_15

Wang B-C, Yee E, Bergstrom DJ (2006) Geometrical description of subgrid-scale stress tensor based on Euler axis/angle. AIAA J 44(5):1106–1110. https://doi.org/10.2514/1.19803

Wilczak JM, Oncley SP, Stage SA (2001) Sonic anemometer tilt correction algorithms. Bound-Layer Meteorol 99(1):127–150. https://doi.org/10.1023/A:1018966204465

Wohlfahrt G, Klumpp K, Soussana J-F (2012) Eddy covariance measurements over grasslands. In: Aubinet M, Vesala T, Papale D (eds) Eddy covariance: a practical guide to measurement and data analysis. Springer Netherlands, Dordrecht, pp 333–344. https://doi.org/10.1007/978-94-007-2351-1_13

Wutzler T, Lucas-Moffat A, Migliavacca M, Knauer J, Sickel K, Šigut L et al (2018) Basic and extensible post-processing of eddy covariance flux data with REddyProc. Biogeosciences 15(16):5015–5030. https://doi.org/10.5194/bg-15-5015-2018

Wyngaard JC, Coté OR, Izumi Y (1971) Local Free Convection, Similarity, and the Budgets of Shear Stress and Heat Flux. J Atmos Sci 28(7):1171–1182. https://doi.org/10.1175/1520-0469(1971)028%3c1171:LFCSAT%3e2.0.CO;2

Xu F, Wang W, Wang J, Huang C, Qi Y, Li Y, Ren Z (2019) Aggregation of area-averaged evapotranspiration over the Ejina Oasis based on a flux matrix and footprint analysis. J Hydrol 575:17–30. https://doi.org/10.1016/j.jhydrol.2019.05.011

Zhang X-Y, Trame MN, Lesko LJ, Schmidt S (2015) Sobol sensitivity analysis: a tool to guide the development and evaluation of systems pharmacology models. CPT Pharmacomet Syst Pharmacol 4(2):69–79. https://doi.org/10.1002/psp4.6